

## Chapter 2

# High-Order Harmonic Generation (HHG)

### 2.1 Introduction

If a material absorbs  $n$  soft photons (with photon energy  $\hbar\omega$ ) and emits one hard photon with energy of  $n\hbar\omega$ , the process is called harmonic generation (HG). In a relatively weak laser field, the harmonic yield decreases as the harmonic order increases. In the higher laser intensity region, the typical harmonic shows first a decline, then reaches a plateau, followed by a sharp cut-off, as shown in figure 2.1. In most of the time, we call the HG in the plateau as a high-order harmonic generation (HHG).

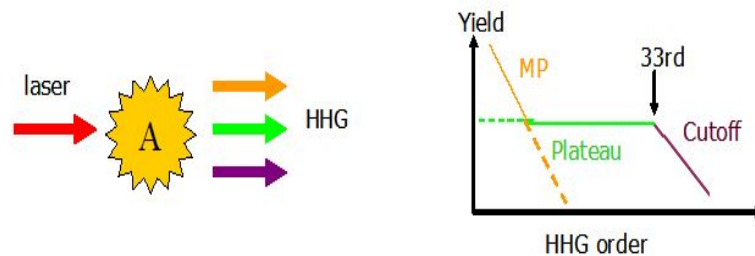


Figure 2.1: Laser interaction with material (left) and the general pattern of the HHG (right).

The HHG was first observed by M. Ferray *et al.*, [1] by using high intensity laser hitting a rare gas target. They observed HG as high as 33<sup>rd</sup>. Their laser parameters are 1064 nm @ 30 ps with  $I = 10^{13} \sim 10^{14}$  W/cm<sup>2</sup>.

The highest HHG observed so far is 297<sup>th</sup> by Z. Chang *et al.*, [2] by using a short pulsed laser on He gas. The laser parameters are 800 @ 26 fs. They obtained the HHG energy as high as 460 eV, which is in the “water window” (2.33 – 4.33 nm) regime. “Water window” refers to the x-ray energy between the C and O K-shells. The x-ray in this energy region can be used to observe DNA structure, the action of viruses and drugs on cells.

## 2.2 Explanation of HHG by the rescattering model

Since the early discovery of the HHG, there have been a lot of theoretical efforts to explain the mechanism of the formation of HHG. Here we will discuss the rescattering model suggested by P. Corkum [3]. This is a three-step model as show in Fig. 2.2:

- electron tunneling out due to the laser field suppressing the potential barrier;
- the tunneling electron bounced back by the laser field;
- emission of HHG by radiative recombination (RR) process.

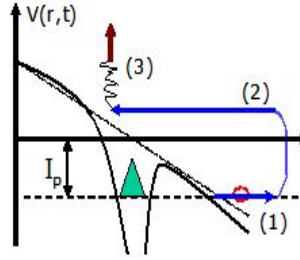


Figure 2.2: Three steps in the rescattering model.

Based on this model, the electron tunnels out at  $t_b$  and returns back at  $t_r$  (left) with the energy spectra  $P(E)$  (middle) in Fig. 2.3. The HHG spectra (right in Fig. 2.3 for a given order  $n$ ) can be expressed as

$$d(n\omega_0) = \langle \phi_g | z | \phi_c \rangle + c.c. \quad \phi_c = Ae^{ip_z z} \quad (2.1)$$

$$A^2 = \int_{(n-1)\hbar\omega_0}^{(n+1)\hbar\omega_0} P(E) dE \quad (2.2)$$

Thus the power spectra  $P(n\omega_0) \propto |d(p)|^2 A^2$  with  $d(p)$  the dipole matrix.

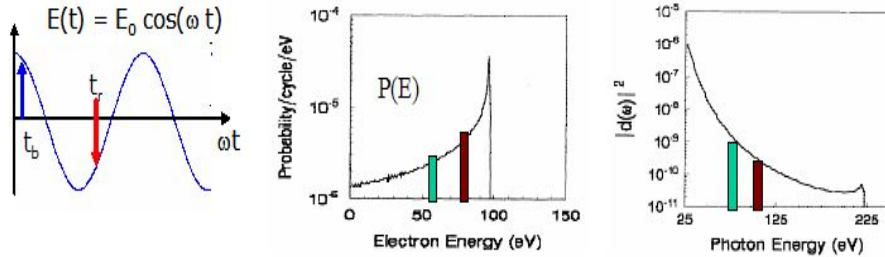


Figure 2.3: Laser field (left), return electron energy spectra (middle), and HHG power spectra (right) calculated from the rescattering model.

This model successfully predicts the HHG cut-off at  $n_c \hbar\omega = I_p + 3.17U_p$  with  $U_p = I_{eff}/(4\omega_0^2)$ , but *fails* to explain the plateau structure. Note here we use  $I_{eff} = \min(I, I_s)$ , with  $I_s$  being the saturation intensity.

## 2.3 Bremsstrahlung and radiative capture processes

When an electron is accelerated or decelerated, it will emit a radiation or photons. This process is called Bremsstrahlung process. In a Coulomb field, the electron can be captured and emits radiation as well. This is called radiative capture as shown in Fig. 2.4. They are expressed as:

$$e + A^{q+} \rightarrow \begin{cases} e' + A^{q+} + \hbar\omega & \text{Brem.;} \\ A^{(q-1)+} + \hbar\omega & \text{RR.} \end{cases} \quad (2.3)$$

Generally radiations from Bremsstrahlung and radiative capture are small except for high

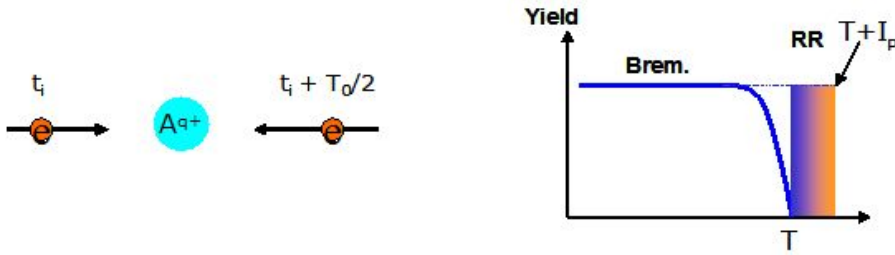


Figure 2.4: The rescattering electron hit the parent ionic core (left) and the Bremsstrahlung and RR spectra (right).

energy electrons colliding with heavy atoms. For lower energy electrons their contributions can be large when the current density is large. Let us estimate the rescattering electron beam current density: Assume the the tunneling probability is  $10^{-4}$  and the electrons returns within a radius  $r_s$  which is taken to be one atomic unit. For 1fs pulse, this means the current density is  $J_e = 10^{-4}/(\pi r_s^2 fs) \simeq 10^8$  A/cm<sup>2</sup>, which is much larger than the electron beam current density we can obtain in the laboratory ( in an EBIS,  $< 10^4$  A/cm<sup>2</sup>). This shows that the Bremsstrahlung and radiative capture probability ( $P \propto \sigma_b J_e \sigma_b$  the Bremsstrahlung cross section) cannot be neglected.

To estimate the radiative yield, recall that the electron beam hits the ion target from left or right at each half cycle as shown in Fig. 2.4 (left). The x-ray spectra should be obtained from the coherent sum of the amplitude of each collision. For a given electron collision energy  $E$ , the radiative spectra can be expressed as

$$P(\omega) \propto \left| \sum_j C(E) (-1)^j e^{-i\omega t_j} \right|^2 \propto \frac{\sin^2(Nx)}{\sin^2 x} \quad (2.4)$$

$$t_j = jT_0/2 + \delta, \quad x = (\omega T_0/2 + \pi)/2 = n\pi \quad (2.5)$$

$$\omega = (2n - 1) \frac{2\pi}{T_0} = (2n - 1)\omega_0 \quad (2.6)$$

where  $C(E)$  is the amplitude of emitting a photon with frequency  $\omega$ . Note that the collisions occur at well-defined times separated by  $T_0/2$  where  $T_0$  is the laser period. By using the rescattering model, combined with the Bremsstrahlung process, we can clearly explain

- only the odder harmonic exist;
- the cut-off is decided by the RR process of the highest returning energy;
- below the cut-off, the HHG yields are almost a constant (Bremsstrahlung spectra is relatively flat away from the cutoff).

This explanation was first suggested by M. Protopapas *et al.*, [4].

## 2.4 HHG power spectra from *ab. initial* calculation

The HHG power spectra can be studied by directly solving the time-dependent Schrödinger equation as

$$i \frac{\partial \Psi(\mathbf{r}, t)}{\partial t} = \left[ -\frac{\nabla^2}{2} + V(\mathbf{r}) - \mathbf{r} E f(t) \right] \Psi(\mathbf{r}, t). \quad (2.7)$$

With the time-dependent wave function, we can calculate the induced dipole

$$d(t) = \langle \Psi(\mathbf{r}, t) | \mathbf{r} | \Psi(\mathbf{r}, t) \rangle \quad \text{length form;} \quad (2.8)$$

$$d_a(t) = \langle \Psi(\mathbf{r}, t) | -\frac{\mathbf{r}}{r^3} - \mathbf{F} f(t) | \Psi(\mathbf{r}, t) \rangle \quad \text{acceleration form} \quad (2.9)$$

The HHG power spectra can be obtained by the Fourier transformation as

$$P(\omega) = \left| \frac{1}{t_f - t_i} \int_{t_i}^{t_f} d(t) e^{-i\omega t} \right|^2, \quad \text{or} \quad P_A(\omega) = \left| \frac{1}{t_f - t_i} \frac{1}{\omega^2} \int_{t_i}^{t_f} d_A(t) e^{-i\omega t} \right|^2. \quad (2.10)$$

Fig. 2.4 shows the calculated time-dependent dipole in length and acceleration forms and the corresponding power spectra.

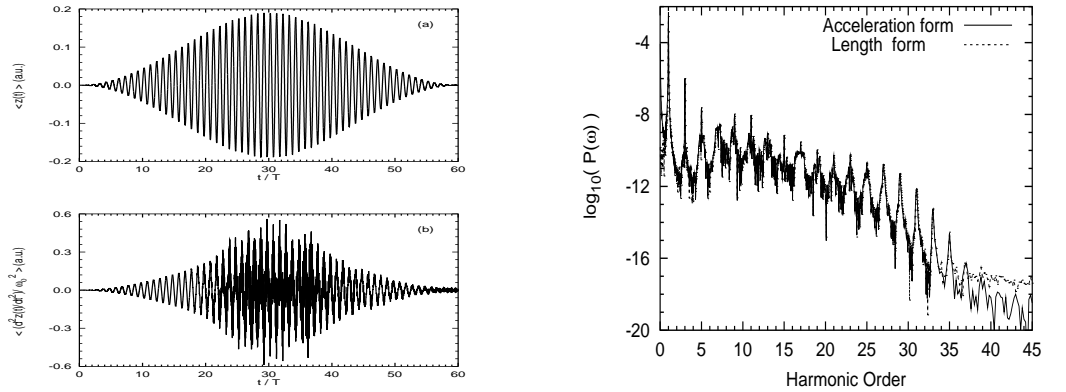
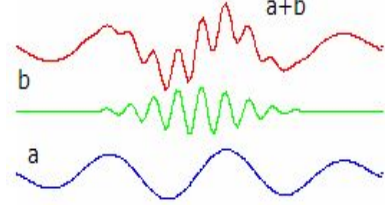


Figure 2.5: Laser induced dipole  $d(t)$  in length (left up), acceleration (left lower) formula, and power spectra (right).  $I = 5 \times 10^{13}$  W/cm<sup>2</sup>, 1064 nm. Details can be found at Ref. [5].

The HHG power spectra calculated by solving the time-dependent Schrodinger equation is in reasonable agreement with the experiment. Did we dig out more physical information from the calculation ? *Not yet.*

## 2.5 Wavelength Analysis

If we know a function  $f(t)$  as shown in the right figure, how can we decompose it into two functions  $f_a(t)$ ,  $f_b(t)$ ? Each of the  $f_a(t)$ ,  $f_b(t)$  has a special character or pattern. Here apart the function  $f(t)$ , we also have additional information, the pattern, in mind. Therefore, we can decompose the  $f(t)$  as  $f(t) = \langle f_a(t) | f(t) \rangle f_a(t) + \langle f_b(t) | f(t) \rangle f_b(t)$  if  $f_a(t), f_b(t)$  are orthogonal.



For HHG, if we know the time-dependent dipole  $d(t)$ , we know the power spectra  $|d(\omega)|^2$  emitted from this dipole oscillator by making a Fourier transformation. Can we ask *when* a given HG is emitted? The time-dependent dipole, which corresponds to the emission of the  $(2n+1)$  order HHG, can be written as

$$d_{2n+1}(t) = \int_{2n\omega_0}^{(2n+2)\omega_0} d(\omega) e^{i\omega t} d\omega. \quad (2.11)$$

In a more general way, we can rewrite the above equation as

$$d_\omega(t) = \int d(t') w_{t,\omega}(t') dt' \quad (2.12)$$

with  $w_{t,\omega}(t') = \sqrt{\omega} W(\omega(t' - t))$ . Note  $W(\omega(t' - t))$  is called mother wavelet.

The physical meaning of the transformation is that we have a window function, we try to find at a time  $t$ , what is the component of  $d(t')$  within this window function, or pattern. Here we choose Morlet wavelet

$$W(x) = \frac{1}{\sqrt{\tau}} e^{ix} e^{-x^2/2\tau^2}, \quad (2.13)$$

which is a natural choice of the light pulse. If  $\tau \rightarrow \infty$ , we get the Fourier transformation. We lose the time information again since the window is too big.

## 2.6 Time-frequency profile

Figure 2.6 (up) shows the time-profile for a HHG near the cutoff region obtained from the wavelet analysis. The quantum calculated results clearly show that the HHG is emitted at the classic returning time for the cutoff HHG. In the plateau regime, the HHG emitted from two classical trajectories, pre- and post returning. This is also consistent with the rescattering model.

Figure 2.6 (lower) shows the time-frequency profile, which support the Bremsstrahlung emission argument. The time-profile of the HHG from MPI is a smooth function of the time while the time-profile of the HHG from the rescattering process contains a lot of bursts (many Bremsstrahlung emissions).

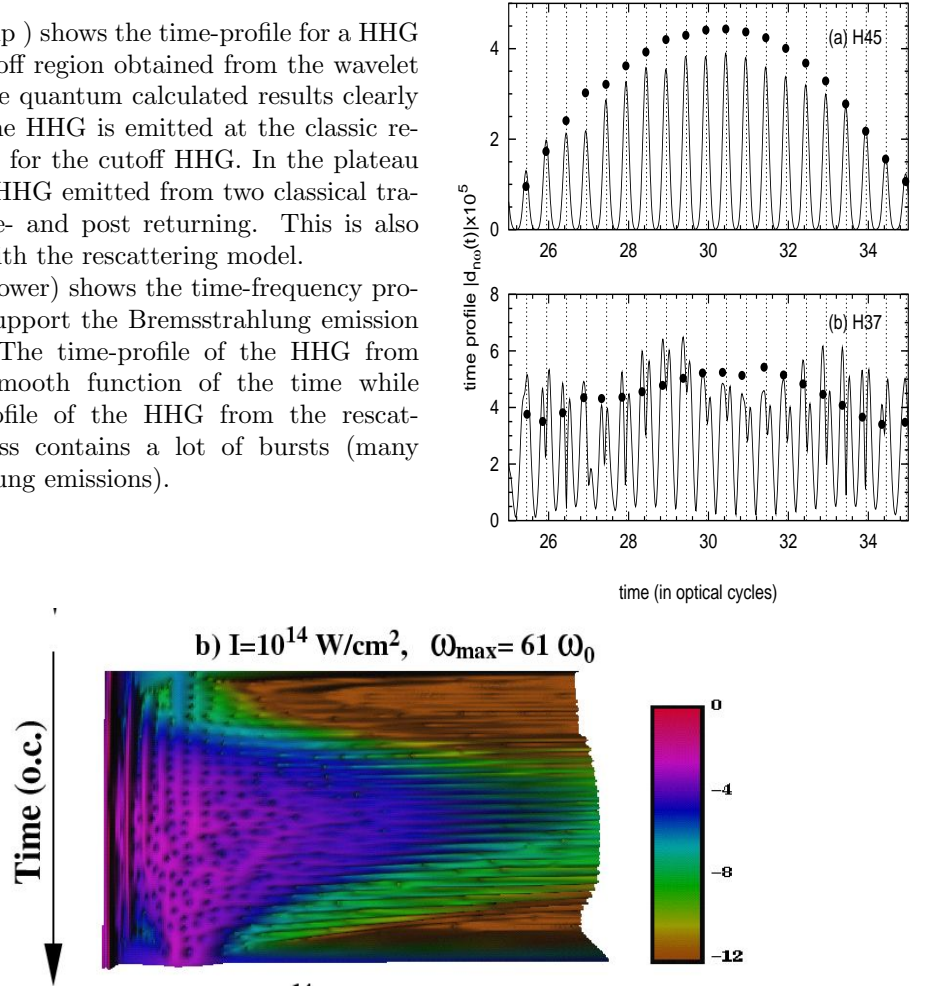


Figure 2.6: Time-frequency profile of the HHG from Ref. [6].

## Summary

Based on the wavelet analysis and an *ab. initial* calculation, we confirm the three step model: (1) tunneling ionization; (2) Back scattering by the laser field; and (3) Revisit the nucleus and emitted a harmonic.

Meanwhile, the wavelet method provides a further understanding: (1) Bremsstrahlung radiation in each re-scattering; (2) Coherent addition of each re-scattering; (3) Blue and red shifts of HHG; and (4) HHG in the plateau and cutoff regions.

## 2.7 HHG from MPI or rescattering

So far, we have understand that the HHG may come from MPI or rescattering processes. The wavelet analysis tells us that time-profile of the HHG from MPI is a smooth function of time and that of the HHG from rescattering contains a lot of bursts in the time domain. The HHG from MPI decreases monotonically as the HHG order increase and the HHG from rescattering process does not very sensitive to the HHG order. Following, we design a two-color cross beam experiment [7] to separate the two process. The experimental setup is shown in figure 2.7.

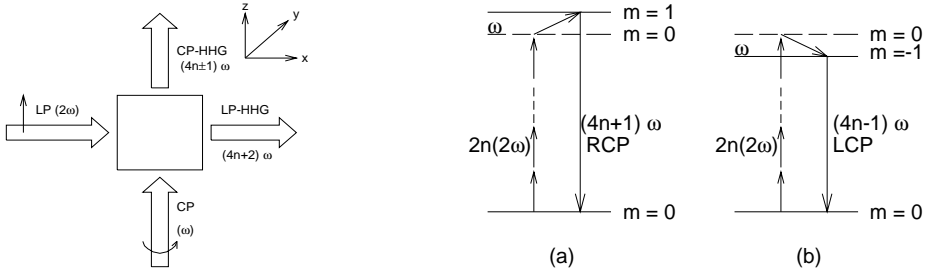


Figure 2.7: Schematic setup for the HHG in the two-color laser field.

As we know, the pure circular polarized laser does not produce the HHG. This can be well understood from the selection rule. From the rescattering model, the tunneling electron will never come back to the parent ionic core. When we add a circular laser to the linear polarized laser field. The circular field does not affect the multi-photon process much. But the circular field will modify the tunneling electron trajectory. Thus we can modify the HHG spectra comes from rescattering electron by tuning the circular laser intensity.

Fig. 2.7 shows the HHG spectra as a function of the circular laser intensity. For a weak circular field, the HHG spectra are close to that of the pure linear polarized field as shown in Figs. 2.7(a) and (b). When the circular laser intensity increases, the peak intensity of the HHG does not changes much ( Fig. 2.7(c) ), but the background of the HHG drops dramatically. As the circular laser intensity increases further, we think most of the tunneling electron can not come back to their parent ionic core and there is not contribution of HHG from the rescattering electron. The remain HG spectra comes from the multiphoton process.

So far, this is a theoretical prediction. We have to take into account the phase matching and other effects in the experiment. Anyway, with the suggested experiment, we can

- CP and LP HHGs are separated;
- Almost pure circular polarized HHG is produced;
- The background can be suppressed by circular laser;
- The CP and LP HHGs can be controlled;
- Better understanding the mechanisms of HHG;

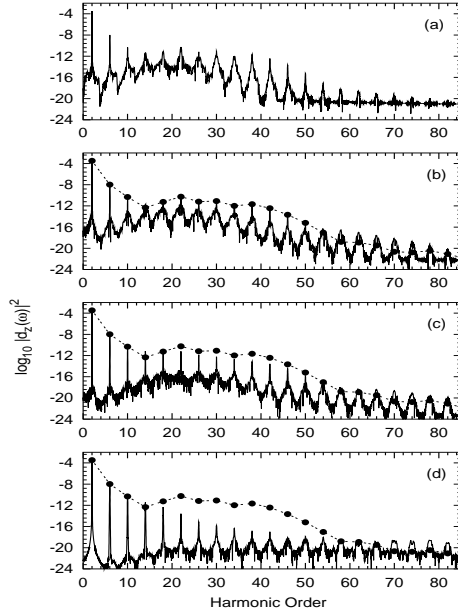


Figure 2.8: HHG in a crossed two colors laser field. (a) No CP field, (b) 1% CP field, (c) 10% CP field, and (d) equal CP and LP field.

By introducing the CP laser, we clearly eliminate the HHG from rescattering electron, which can be explained well within rescattering Model.

We can also modify the rescattering electronic trajectory by adding a static magnetic field [8]. Unfortunately, the required magnetic field is too strong, which can not be provided in the laboratory.

## 2.8 Lewnstein Model for HHG

In principle, we can obtain the HHG spectra by solving the time-dependent Schrödinger equation. This will take a lot of computer efforts and does not provide much physical insight. Moreover, we need some simple model which can be easily used by most of experimentalists. Lewenstein *et al.* [9] suggested a simple model based on the rescattering picture and the strong field approximation (SFA). We will brief the physical ideal of their model without going through the numerical detail.

The solution of the time dependent Schrödinger equation,

$$i \frac{\partial \Psi(\mathbf{r}, t)}{\partial t} = \left[ -\frac{\nabla^2}{2} + V(\mathbf{r}) - \mathbf{r} E f(t) \right] \Psi(\mathbf{r}, t), \quad (2.14)$$

$$H = T + V_n(\mathbf{r}) + V_f(t), \quad (2.15)$$

can be expressed formally as

$$|\Psi(t)\rangle = U(t, -\infty) |\Phi_o\rangle, \quad \text{with} \quad (2.16)$$

$$U(t, t') = e^{-i \int_{t'}^t H d\tau}. \quad (2.17)$$

It can be further expressed as

$$\begin{aligned} |\Psi(t)\rangle &= U(t, t_1)U(t_1, -\infty)|\Phi_o\rangle \\ &= \sum_m U(t, t_1)|\Phi_m\rangle \langle \Phi_m|U(t_1, -\infty)|\Phi_o\rangle \end{aligned} \quad (2.18)$$

So far, the formal solution is exact and equivalent to solve the time-dependent Schrödinger equation. Following approximations are made to propagate the electronic wavefunction;

- No other bound states in the summation over the intermediate states,
- No depletion of  $\Phi_o$ ,
- Free electron only moving in the laser field.

With this three approximations, the time-dependent wave function can be expressed as

$$|\Psi(t)\rangle = \int U(t, t_1)|\mathbf{p}\rangle \langle \mathbf{p}|U(t_1, -\infty)|\Phi_o\rangle d\mathbf{p} \quad (2.19)$$

$$= \int d\mathbf{p}U(t, t_1)|\mathbf{p}\rangle \mathbf{d}(\mathbf{p})C(\mathbf{p}, t_1)dt_1 \quad (2.20)$$

$$C(\mathbf{v}, t) = \int_{-\infty}^t \mathbf{E}(\tau)e^{i(\mathbf{p}^2/2 - \epsilon_o)\tau} d\tau, \quad (2.21)$$

$$\mathbf{d}(\mathbf{p}) = \langle \mathbf{p}|\mathbf{r}|\Phi_0\rangle \quad (2.22)$$

$$U(t, t_1)|p\rangle = e^{-i \int_{t_1}^t (\mathbf{p} - \mathbf{A}(t') + \mathbf{A}(t_1))^2/2 dt'} e^{i(\mathbf{p} - \mathbf{A}(t) + \mathbf{A}(t_1))\mathbf{r}} \quad (2.23)$$

$$\mathbf{A}(t) = \int_{-\infty}^t \mathbf{E}(\tau)d\tau. \quad (2.24)$$

Define  $\mathbf{p}' = \mathbf{p} - \mathbf{A}(t) + \mathbf{A}(t_1)$ , the time-dependent induced dipole can be written as

$$\mathbf{d}(t) = \langle \Psi(t)|\mathbf{r}|\Psi(t)\rangle \quad (2.25)$$

$$= \int d\mathbf{p}\mathbf{d}(\mathbf{p}')U(t, t_1)\mathbf{d}(\mathbf{p})C(\mathbf{p}, t_1)dt_1 + c.c \quad (2.26)$$

The physical meaning of this equation are:

- an electron is promoted into a continuum state by the laser field at  $t_1$  by the dipole interaction
- the electron propagates in the laser field from  $t_1$  to  $t$ ;
- and recombined with parent ionic core by a dipole transition.

To further simplify the equation, we only follow the electron with classical trajectory in the laser field. That means only the electron with  $\mathbf{r} = 0$  at both  $t_1, t$  has contribution to the HHG. This will simplify the integrate over  $\mathbf{p}$  a lot.

Note that limitation of no depletion can be removed by introducing a decay rate for the ground state. Meanwhile, this model basically works well for initial state with  $m = 0$ . It fails for other  $m$  due to only the leading term in the classical trajectory has contribution and there is no electron in the field direction with  $m \neq 0$ .

# Bibliography

- [1] M. Ferray *et al.*, J. Phys. B **21**, L31 (1988).
- [2] Z. Chang *et al.*, Phys. Rev. Lett. **79**, 2967 (1997).
- [3] P. B. Corkum, Phys. Rev. Lett. **71**, 1994 (1993).
- [4] M. Protopapas, D. G. Lappas, C. H. Keitel, and P. L. Knight, Phys. Rev. A **53**, R2933 (1996).
- [5] X. M. Tong and S. I. Chu, Chem. Phys. **217**, 119 (1997).
- [6] X. M. Tong and S. I. Chu, Phys. Rev. A **61**, 021802 (2000).
- [7] X. M. Tong and S. I. Chu, Phys. Rev. A **58**, R2656 (1998).
- [8] X. M. Tong and S. I. Chu, J. Phys. B-At. Mol. Opt. Phys. **32**, 5593 (1999).
- [9] M. Lewenstein *et al.*, Phys. Rev. A **49**, 2117 (1994).